Magnetization reversal properties of Fe/NiO/Fe(001) trilayers

A. Brambilla,* P. Biagioni, M. Portalupi, M. Zani, M. Finazzi, and L. Duò
INFM, Dipartimento di Fisica, Politecnico di Milano, Piazza Leonardo Da Vinci 32, 20133 Milano, Italy

P. Vavassori
INFM, S[3], Dipartimento di Fisica, Università di Ferrara, Via Paradiso 12, 44100 Ferrara, Italy

R. Bertacco and F. Ciccacci†
L-NESS, Dipartimento di Fisica, Politecnico di Milano, Via Anzani 52, 22100 Como, Italy
(Received 5 August 2004; revised manuscript received 4 August 2005; published 1 November 2005)

We have investigated the magnetic properties of epitaxially grown Fe/NiO/Fe(001) trilayers for different thickness combinations of the NiO spacer and of the Fe overlayer. The magneto optical Kerr effect has been exploited to study the in-plane magnetization reversal processes in the iron layers. Further information has been obtained by means of spin polarized inverse photoemission spectroscopy. We show the existence of a critical value t_c of the NiO thickness t_{AFM} for the magnetic coupling between the Fe layers at zero applied field: for $t_{AFM}<t_c$ the magnetization directions align perpendicularly, while the alignment is collinear for thicker spacers. A phenomenological model has been developed to reproduce the reversal properties of the trilayer and determine the dependence of the coupling energy between the Fe ferromagnetic layers as a function of their relative orientation. We find that the observed behavior cannot be reproduced by a Slonczewski's coupling term, but rather it is obtained when a biquadratic term is employed.

DOI: 10.1103/PhysRevB.72.174402 PACS number(s): 75.60.Jk, 75.70.Cn, 75.25.+z, 75.50.Ee

I. INTRODUCTION

The coupling between ferromagnetic (FM) layers separated by a nonferromagnetic spacer has recently attracted a great deal of attention. The challenge to find an exhaustive model describing the magnetic coupling mechanism is still open. Furthermore, the unique properties of such systems are also appealing in view of the possible applications to, e.g., magnetic sensors and magnetic recording devices.[1]

The case of trilayers where two FM films are separated by a thin insulating antiferromagnetic (AFM) spacer can be of great interest, because the indirect interaction due to conduction electrons is ruled out, and one would expect a large contribution coming from direct nearest-neighbor exchange across the spacer and the interfaces. Moreover, the phenomenology of FM/AFM interfaces can potentially include the well-known exchange bias effect.[2] A satisfactory agreement between theory and experimental results on such FM/AFM/FM trilayers is, at present, not yet achieved. In particular, both collinear[3,4] and perpendicular[5–9] alignment between the magnetization directions in the FM layers at zero applied field have been reported in the literature. In some cases, systems where NiO is chosen as an AFM spacer show a 90° relative orientation.[8,9] Several theoretical and phenomenological models have been developed in order to explain and simulate the noncollinear alignment between the magnetization directions of the two FM layers.[10–12] It is now clear that, when the spacer is antiferromagnetic, the exchange coupling with the FM layers at the interfaces and the spin structure of the spacer play a very important role.

A further incentive for the analysis of the Fe/NiO/Fe trilayers is given by the fact that different magnetic behaviors have been reported for the Fe/NiO bilayer[13] and the reverse NiO/Fe case.[14] This situation could be explained on the basis of different growing processes as well as different chemical reactions at the interfaces,[15] as it was also underlined in analogous systems.[3]

Here we report on measurements of the magnetic properties of Fe/NiO/Fe(001) trilayers, epitaxially grown on MgO(001) substrates. The interlayer coupling between Fe/NiO/Fe trilayers has been systematically investigated by spin polarized inverse photoemission spectroscopy (SPIPE), performed *in situ* on freshly prepared samples. The coupling has been studied as a function of both the NiO spacer and the Fe overlayer thickness, t_{AFM} and t_{over}, respectively. On the basis of the phase diagram obtained by SPIPE, we prepared a subset of samples with different t_{AFM} values characterizing distinct qualitative magnetic behaviors of the trilayer, and we investigated their magnetization reversal processes exploiting the magneto optical Kerr effect (MOKE).

MOKE and SPIPE results suggest that 90° domains nucleate and are energetically favorite for trilayers with t_{AFM} lower than a critical value t_c, while collinear coupling has been observed for the cases with a thicker spacer. A phenomenological model based on a biquadratic coupling term[10] has been used to interpret the observed loops. The model and the consequent results will be discussed in detail and compared to the experimental data.

II. SAMPLE PREPARATION

Fe(001)/NiO(001)/Fe(001) samples were prepared in an ultrahigh vacuum chamber (5×10^{-11} Torr base pressure), starting from a thick (>3000 Å) iron film, grown by molecular beam epitaxy (MBE) on a MgO(001) single crystal substrate, 1 cm^2 wide. As reported elsewhere,[16] annealing such a film up to about 900 K produces high quality bulklike samples with a sharp (1×1) low energy electron diffraction pattern and no contamination detectable with surface

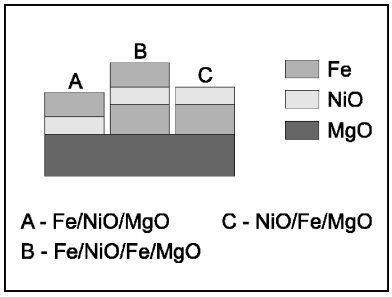

FIG. 1. Sketch of prepared samples. The dimensions and positions of the layers are not representative of the real setup.

analysis techniques. The sample was then exposed to oxygen, in order to obtain the very stable and well-characterized Fe(001)-p(1×1)O surface.[17] This precaution lowers the possibility of uncontrolled oxidation of the substrate surface due to the high exposure to O_2 needed to prepare the spacer films, as described below, and thus assures a good reproducibility of the growth conditions of NiO. The Fe(001)-p(1×1)O surface also shows enhanced spin dependent effects.[17] This film has been remanently magnetized along the [100] Fe in-plane easy axis before growing the NiO layer.

The NiO thin film was grown by evaporating metal Ni by means of electron bombardment, at a rate of about 2 Å per minute, in an oxygen partial pressure $p_{O_2}=7.5\times10^{-7}$ Torr. Samples were prepared with the spacer thickness varying between 4 and 100 Å. The good quality of the NiO films has been confirmed by x-ray photoemission spectroscopy (XPS) and inverse photoemission spectroscopy.[18] Within the sensitivity of these two techniques, no defect states in the gap have been detected, fixing the upper limit of the density of defects in the NiO films to a few percent.

Thin Fe overlayers with thickness ranging from 14 Å to 140 Å were grown on top of NiO by MBE. The unequal coercive fields of the two Fe layers, as expected on the basis of their quite different thicknesses, allows one to easily separate their contributions in the hysteresis loops. The thicknesses of the iron layers and of the nickel oxide spacer are such that the former are ferromagnetic while the latter is antiferromagnetic at room temperature.

Finally, for *ex situ* MOKE measurements, samples were capped with about 20 Å of Au in order to prevent oxidation. SPIPE spectra were instead collected *in situ* on noncapped samples.

For MOKE analysis, conveniently shaped mechanical masks were used to prepare samples where, besides the described trilayer, even the intermediate structures were present. Measurements could then be performed on the trilayers and also on Fe/NiO/MgO and NiO/Fe/MgO bilayers, on the same sample. This possibility has shown to be useful to precisely define the values for some of the parameters involved in the numerical simulations. It is worth noting that NiO grows on MgO(001) and on Fe/MgO(001) with a similar crystal structure, due to the low lattice mismatches.[18,19] An outline of the prepared samples is reported in Fig. 1.

The thickness of the various layers was calibrated during each sample preparation step by means of a quartz microbalance, while the stoichiometry of the sample was correspondingly monitored with XPS. The angle between the sample surface normal and the direction of the molecular beam was 25° for all depositions.

III. MOKE

A. Experiments

MOKE vector magnetometry has been performed to obtain hysteresis loops of the samples and thus characterize their magnetic behavior.[20] Due to the large penetration depth of the photons compared to the low thickness of the Fe overlayer and NiO spacer, the magnetization reversal behavior of both FM layers is probed. In order to get a detectable signal from the upper iron layer, only samples with a thick enough overlayer have been used. Namely, an overlayer thickness of 70 Å has been chosen for each of the samples prepared for MOKE, and only the NiO thickness has been varied. The measurements have been performed at room temperature, applying an external magnetic field **H** along one of the in-plane easy axes of the iron overlayer. Both the longitudinal and transverse hysteresis loops have been collected giving information, respectively, on the in-plane parallel and perpendicular components of the layers' magnetizations with respect to the applied field **H**. No out-of-plane component of the magnetization vector has ever been observed.

B. Results and discussion

In analyzing the results of the MOKE measurements and the numerical simulations, each of the following structures will be considered: the NiO/Fe bilayer, the Fe/NiO bilayer, and the Fe/NiO/Fe trilayer. Hereafter we will employ a reference system with the x, y, and z axes parallel to the [100], [010], and [001] Fe crystal directions, respectively, with [001] being the normal to the layers. The x and y axes defined in this way also coincide with the Fe in-plane easy magnetization directions.

Starting with the NiO/Fe bilayer, no effect that could be ascribed to interface exchange bias has been detected on the Fe substrate after room temperature NiO deposition. Neither horizontal shift of the hysteresis loops, nor significant variations of the coercive field were observed. When **H** is applied along an easy axis, the hysteresis loops (not shown) present sharp transitions and a square shape, with a small coercive field of about 5 Oe. The iron anisotropy is in-plane with a fourfold symmetry around the sample normal. No significant change in the magnetization reversal behavior of the substrate seems to be induced by the NiO overlayer. This is not surprising due to the large thickness of the Fe substrate and to the very small thickness and low magnetocrystalline anisotropy of the NiO layer.[21] An exchange bias can be induced, in principle, by field cooling the sample across its Néel temperature. However, such a thermal treatment is not possible in this case because of a thermally driven substitution reaction occurring at the NiO/Fe interface.[18]

Coming next to the Fe/NiO bilayer, the longitudinal loop obtained with $\mathbf{H}\|x$ (measuring M_x) is characterized by sharp transitions and a coercivity of about 15 Oe [Fig. 2(a)], while

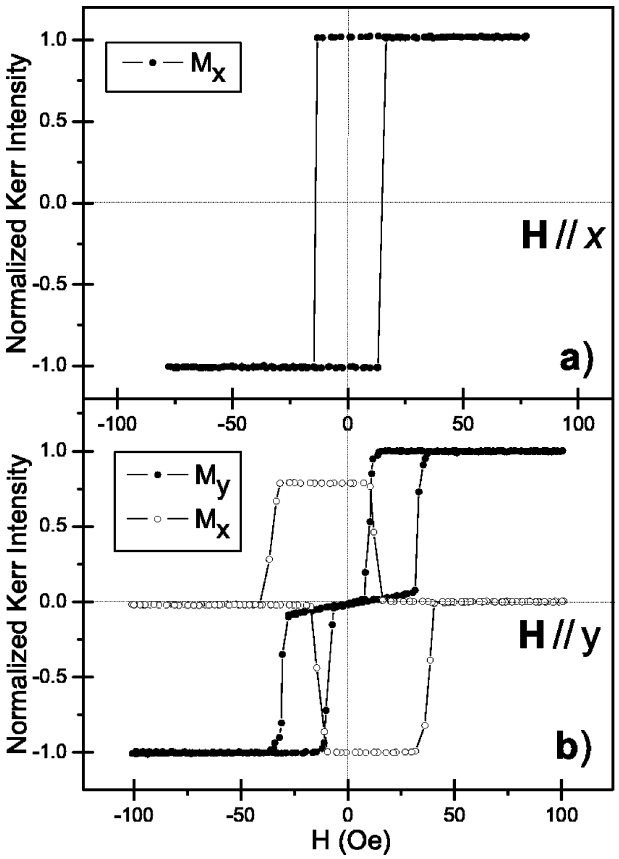

FIG. 2. Experimental hysteresis loops for the overlayer in the Fe(70 Å)/NiO(14 Å) bilayer. Loops have been normalized to unity. The field is applied first along the x axis (upper panel) and then orthogonally to it, along the y axis (lower panel).

for $\mathbf{H}\|y$ a *two-step* longitudinal loop (measuring the M_y component) appears [Fig. 2(b)]. This behavior has been interpreted as due to a small uniaxial anisotropy in the thin layer,[22] with its easy axis parallel to x, superimposed to the cubic intrinsic anisotropy. The uniaxial anisotropy makes the two cubic axes no longer equivalent and stabilizes the intermediate metastable state where, if the applied $\mathbf{H}$ is perpendicular to the uniaxial easy axis, the spins are directed perpendicularly to their saturation directions. The M_x measurement acquired with $\mathbf{H}\|y$, also plotted in Fig. 2(b), confirms this interpretation, showing a transverse component of the magnetization vector at correspondence with the central plateau in the longitudinal loop. No significant M_y component for $\mathbf{H}\|x$ has ever been observed. We attribute the uniaxial anisotropy to the oblique incidence of the beam during NiO deposition: this can generate a uniaxial strain, which influences the magnetic properties of the system via the large NiO magnetostriction.[9,23] The different heights of the two plateaux observed in the transverse loop of Fig. 2(b) can be explained by assuming the presence of both +90° and −90° domains in the Fe overlayer resulting in a total M_x signal reduced with respect to the saturation value. The height of the plateau in each branch, hence the partition between ±90° domains, is random, i.e., is not reproduced in successive hysteresis loops.

As anticipated above, a simple phenomenological model based on coherent rotation of the magnetic moments has been developed in order to simulate the FM magnetization reversal of our system and get a better insight in the physics involved.

The related numerical simulations are based on energy minimization, taking into account the intrinsic energy terms for the FM layers, their interaction energy with the applied field and, for the trilayers, the phenomenological terms describing the Fe-Fe coupling across the AFM spacer (see below). The hypothesis underlying the simulation is that, once a domain has been nucleated, a very small increase in the applied field $\mathbf{H}$ will suffice to make it propagate freely, so that the sample can always be considered to be in a single-domain state. Actually, as noted above, the different heights of the M_x plateaux in Fig. 2(b) indicate that the real overlayer can indeed be in a multidomain state. However, the sharpness of the observed transitions in the experimental hysteresis loops indicates that domain walls do rapidly span large portions of the overlayer before being pinned by defects.[22] By applying the single-domain model described above we deliberately chose to neglect domain wall pinning after nucleation. This pinning does not influence the overlayer anisotropy and coercivity, and it just affects the maximum M_x value that can be observed in the transverse hysteresis loops.

For the Fe/NiO bilayer, only the energy of the Fe overlayer is considered, without any coupling term. Both a cubic magnetocrystalline anisotropy and a small uniaxial term superimposed to it are considered for the Fe overlayer. In order to simulate the overlayer hysteresis, energy barriers for nucleation of both 180° and 90° states were included. The values for all the energy barriers are directly taken from the observed experimental loops. We stress that they just affect the nucleation field (giving hysteretic behavior), while the transitions between different alignments are determined by the values of the anisotropy energies and, for the trilayer, by the coupling terms. The simulation procedure was therefore the following: first, anhysteretic loops have been calculated by finding the global minimum for the energy at different values of the external applied field, without any energy barrier. A fitting procedure has then been performed in order to find the best values for the free parameters in the model. Finally, energy barriers have been chosen so as to reproduce the hysteresis of the observed loops.

The total energy per unit surface is the following:

$$E_{\text{over}} = -HM_S t_{\text{over}} \cos(\theta - \phi_1) + \frac{1}{4}K_4 t_{\text{over}} \sin^2(2\phi_1) + K_2 t_{\text{over}} \sin^2(\phi_1),$$

where $\mathbf{H}$ is the applied field, M_S the saturation magnetization (taken to be 1742 emu/cm^3, as in bulk Fe), θ is the angle between $\mathbf{H}$ and the easy x axis, ϕ_1 is the angle between the Fe overlayer magnetization and the x axis. Results for these simulations are shown in Fig. 3. Referring to the simulated longitudinal loop with $\mathbf{H}\|y$ (measuring M_y) in Fig. 3(b), the cubic anisotropy value K_4 directly influences the slope at the origin, while the uniaxial anisotropy term K_2 mainly affects the magnitude of the transition fields between different orientations. A good agreement between the numerical simu-

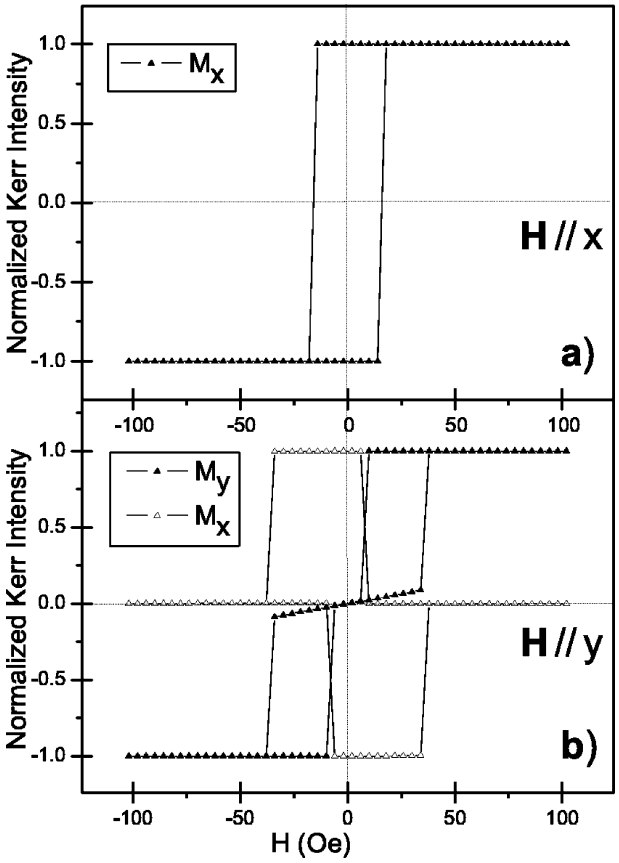

FIG. 3. Simulated hysteresis loops for the overlayer in the Fe(70 Å)/NiO(14 Å) bilayer. Loops have been normalized to unity.

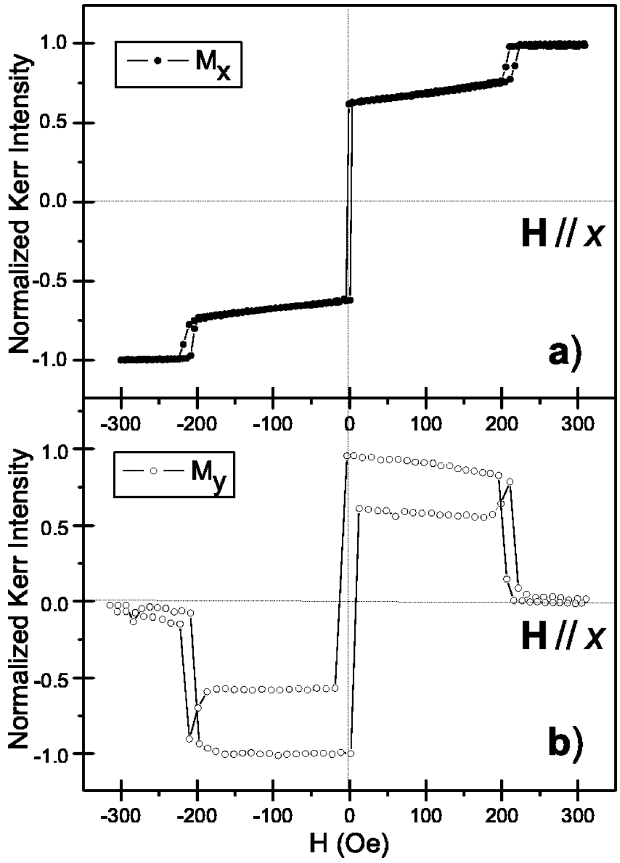

FIG. 4. Experimental longitudinal [panel (a)] and transverse [panel (b)] hysteresis loops for the Fe(70 Å)/NiO(14 Å)/Fe(3000 Å) trilayer ($\mathbf{H}\|x$). Loops have been normalized to unity.

lations of the overlayer magnetic behavior and the experimental data for the Fe/NiO system is obtained with a uniaxial energy constant $K_2=2.94\times10^4$ erg/cm^3 and a value $K_4=2.44\times10^5$ erg/cm^3 for the cubic anisotropy constant. A sensitivity analysis has been carried out applying different values of K_2 and K_4 around the best fit, giving an overall uncertainty for these two parameters of about ±5% and ±1%, respectively.

Let us now discuss the case of the Fe/NiO/Fe trilayers. As outlined by SPIPE results (see below), two distinct Fe-Fe coupling behaviors are observed at correspondence with different interlayer thicknesses, with a critical thickness t_c of about 40 Å for the transition between the two regimes. Figure 4 reports the experimental hysteresis loops obtained for $\mathbf{H}\|x$ on the Fe(70 Å)/NiO(14 Å)/Fe(3000 Å) trilayer, i.e., for $t_{AFM}<t_c$. Both the longitudinal (M_x) and transverse (M_y) loops are shown. In the upper panel of Fig. 4, the inner (low H values) narrow loop, with a coercivity of about 5 Oe, can be attributed to the Fe substrate, while the outer (high H values) loop, with a saturation field of about 230 Oe, comes from the contribution of the thin Fe overlayer. The latter, at low applied fields, has its magnetization oriented perpendicularly to the magnetization of the substrate layer, as confirmed by the transverse hysteresis loop [M_y in Fig. 4(b)], which shows a transverse component of the in-plane magnetization vector at correspondence with the intermediate plateaux of the longitudinal loop. The saturation field for the overlayer is larger in the Fe/NiO/Fe trilayer than in the Fe/NiO bilayer, as a consequence of exchange coupling between the two FM layers across the AFM spacer, as already reported in the literature.[9]

Different samples, with the same nominal combinations of t_{AFM} and t_{over} as above, showed different saturation fields, ranging between 130 and 230 Oe. Furthermore, an increase of about 50% in the saturation field was measured on the same samples about three months after the first measurements, revealing an aging effect despite the Au capping layer. The samples had been stored in a low vacuum (a few mbar) container. However, no differences are observed in the shape of the hysteresis loops, thus excluding any significant change in the physics of the system.

A remarkable feature observed in the transverse loop, as reported in Fig. 4(b), is that the overlayer magnetization **M** reverses when the substrate magnetization changes sign. When the externally applied magnetic field **H** has reached the coercive value, the spins of the Fe atoms in the substrate rotate to align in the direction of the field. In doing so, they seem to exert a drag on the spins of the overlayer, which rotate accordingly conserving the 90° coupling.

This behavior shows analogies with the results of previously unreported experiments that we performed on NiO/Fe bilayers using room temperature x-ray magnetic linear dichroism (XMLD) at the Ni L_2 edge. The data were collected at the beam line BACH at the ELETTRA synchrotron radiation facility in Trieste, Italy.[24] NiO thin films on Fe(001)

develop an in-plane uniaxial anisotropy axis whose direction can be determined in a straightforward manner from the analysis of the XMLD spectra.[14] These have been obtained as the difference between the absorption spectra measured with the x-ray electric field either parallel or perpendicular to the Fe magnetization **M**. We have then compared the mentioned XLMD signals before and after **M** had been rotated from the [100] to the [010] direction. Within the experimental errors we have seen that the XLMD signals are the same. We can therefore conclude that the magnetic anisotropy axis in the NiO epilayer rotates together with the Fe substrate magnetization, with no evidence of AFM domain pinning, most probably as a consequence of interface exchange coupling. In a similar way, we explain the rapid transition of M_y from positive to negative values in the transverse loop by assuming that the Fe epilayer magnetization direction is determined by the coupling to the NiO anisotropy axis, which rotates by 180° during the reversal of the substrate magnetization.

From Fig. 4(b) one may notice that the inversion of the overlayer magnetization **M** at the substrate coercive field is incomplete. M_y reverses sign but settles on a smaller absolute value than before inversion. It appears that the overlayer breaks into several domains coupled at ±90° to the substrate, probably as a consequence of the sudden incoherent reversing of the substrate magnetization at ±5 Oe. This situation remains stable until the magnitude of the externally applied magnetic field approaches the saturation value, where a peak in the transverse loop of Fig. 4(b) indicates that M_y rapidly reapproaches the value observed before the inversion of the substrate.

Similarly to the Fe/NiO bilayer, the value of K_4 can be determined from the slope of the overlayer M_x loop at $\mathbf{H}=0$. We find, by means of a fitting procedure, a value very close to the one used in that case. As for K_2, we find that the uniaxial energy term found in the Fe/NiO bilayer disappears almost totally in the Fe/NiO/Fe trilayers, where it is at least a factor of 10 lower, and the loops measured for $\mathbf{H}\|y$ (not shown) and $\mathbf{H}\|x$ are practically identical.

A simple explanation for the reduction of the uniaxial anisotropy in the trilayer could be that NiO grows differently on MgO and on Fe, therefore inducing a sizable K_2 value in one case, but not in the other. As a matter of fact, the lattice mismatch is negative (−0.9%) for NiO/MgO(001) and positive (+2.8%) for NiO/Fe(001).

In the simulation, the coupling between the two FM layers is described by a bilinear term, favoring collinear alignment, and a biquadratic term, which favors perpendicular alignment.[10] The total energy per unit surface for the Fe/NiO/Fe trilayer is expressed as follows:

$$E_{\mathrm{tri}} = -HM_S t_{\mathrm{sub}} \cos(\theta - \phi_2) + \frac{1}{4} K_4 t_{\mathrm{sub}} \sin^2(2\phi_2)$$

$$- HM_S t_{\mathrm{over}} \cos(\theta - \phi_1) + \frac{1}{4} K_4 t_{\mathrm{over}} \sin^2(2\phi_1)$$

$$+ C_1 \cos(\phi_1 - \phi_2) + C_2 \cos^2(\phi_1 - \phi_2),$$

where t_{sub} is the Fe substrate thickness and ϕ_2 is the angle between the magnetization direction and the x axis in the Fe substrate. The coupling coefficients C_1 and C_2 are free parameters and are fitted to the experimental data. The fitting procedure is the same as before. Note the absence of the uniaxial energy term for the overlayer.

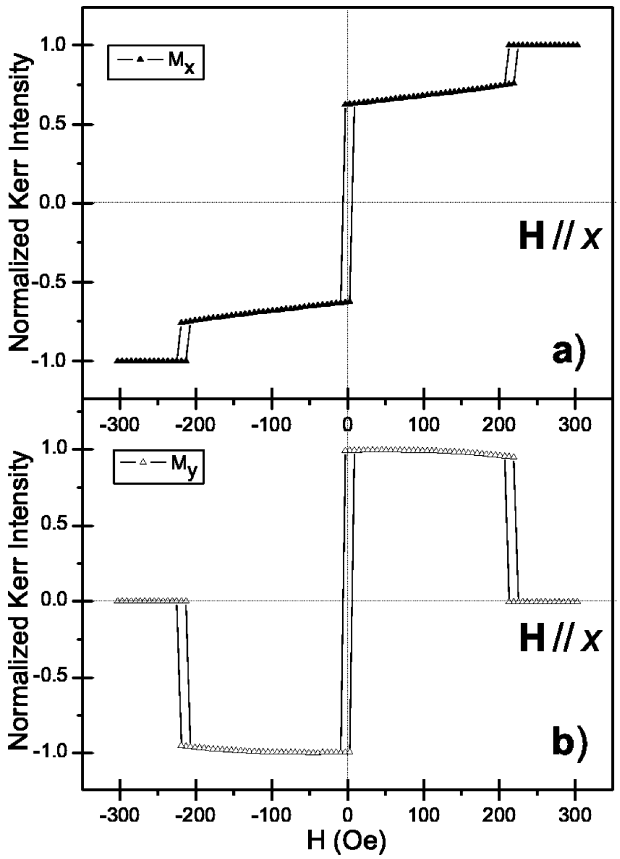

FIG. 5. Simulated hysteresis loops for the Fe(70 Å)/NiO(14 Å)/Fe(3000 Å) trilayer ($\mathbf{H}\|x$). Loops have been normalized to unity.

Because of the large thickness of the substrate, its magnetization direction ϕ_2 is just determined by its magnetocrystal anisotropy and by the interaction with the external magnetic field, while the coupling terms and, hence, the ϕ_1 value have a negligible influence. On the contrary, the coupling plays a fundamental role in defining the reversal properties of the overlayer magnetization.

Numerical simulations for these results are shown in Fig. 5. The best fit is obtained with $C_2 = 1.86 \times 10^{-1}$ erg/cm^2, with an uncertainty of about ±3%. The maximum value of the bilinear coefficient C_1 compatible with the experimental loops is about 5×10^{-2} erg/cm^2, which is nearly three times smaller than C_2. Again, the difference in the height of the plateaux in the experimental and simulated transverse loops [Figs. 4(b) and 5(b), respectively] is due to the fact that our model does not account for the possibility that the Fe overlayer could be in a multidomain state.

In the following, we thoroughly discuss the expression that we have chosen for the coupling terms. First of all, the bilinear term either favors a parallel or antiparallel coupling between the FM layers, depending on the sign of C_1. The

insulating character of NiO allows us to exclude any contribution to the bilinear term due to the Rudderman-Kittel-Kasuya-Yosida (RKKY) interaction. Also, for the NiO thickness range that we have investigated, we do not expect that bilinear coupling related to tunneling phenomena can be of great importance. We attribute the bilinear term to the dipolar coupling between the FM layers, which favors an antiparallel alignment. Our simulations suggest that the bilinear term is small, as it can be expected for a dipolar interaction, with respect to the biquadratic one, which, on the other hand, reflects the interplay between the exchange coupling at the interfaces and across the NiO spacer.

Slonczewski[11] proposed that the perpendicular coupling through an AFM spacer should be described in the frame of the so-called proximity magnetism model by a coupling term of the form $A_1(\phi_1-\phi_2)^2+A_2(\phi_1-\phi_2-\pi)^2$. The main difference between this phenomenological description and one assuming a biquadratic term is the behavior at high applied fields, as the magnetization reaches the saturation value only asymptotically for the Slonczewski term. We tried to use this term in the energy expressions, but, at variance with Ref. 8, we could not reproduce our experimental data, which show a saturation magnetization for finite values of the applied field.

The angular dependence of the coupling term is particularly important since it depends directly on the qualitative behavior of the magnetic moments across the AFM-FM interfaces. Slonczewski's proximity model has been developed for an uncompensated interface and requires strong AFM-FM coupling, as compared to the domain wall energy density.[11] The NiO(001) interface plane is, however, compensated. Nevertheless, Slonczewski's model provides a good description of the results reported in Ref. 8 about $Fe_3O_4/NiO/Fe_3O_4(001)$ since the $Fe_3O_4(001)$ plane has a magnetic lattice parameter that is almost exactly twice (mismatch 0.5%) that of NiO and thus interacts only with one of the two uncompensated sublattices of the NiO(001) interface plane. Despite that Fe_3O_4 is also formed at the interface obtained by depositing NiO on Fe(001),[15] a different oxide, namely FeO, is expected to form when Fe is deposited on NiO(001) to complete the trilayer.[13] The AFM-FM coupling in the Fe/NiO/Fe trilayer can thus be expected to be much lower than in $Fe_3O_4/NiO/Fe_3O_4$, at least at one interface. This provides one reason why a Slonczewski's coupling term is not appropriate to describe our system.

Slonczewski's proximity model has recently been extended to the case where the interfacial coupling and AFM domain wall energy densities are comparable.[12] In the "extended" proximity model the FM-FM coupling energy can be approximated,[12] to lowest order, by a combination of a biquadratic contribution, proportional to $\cos^2(\phi_1-\phi_2)$, and a term proportional to $\sin^2[2(\phi_1-\phi_2)]$.[25] In our experimental hysteresis loops the Fe substrate magnetization is always parallel to an easy axis, therefore the $\sin^2[2(\phi_1-\phi_2)]$ contribution is *de facto* equivalent to an extra cubic anisotropy term of the Fe overlayer. In our simulations we do not make any distinction and use only one free parameter, namely K_4, indicating the weight of a term proportional to $\sin^2(2\phi_1)$.

The angular dependence of the coupling energy explains the different predictions of the extended proximity model concerning the asymptotical behavior of the trilayer. In fact, the trilayer energy obtained when a Slonczewski's term is used only has a mimimum for $(\phi_1-\phi_2)=90°$. On the other hand, using the coupling term predicted by the extended proximity model, we obtain a total trilayer energy which has minima also at $(\phi_1-\phi_2)=0$ or $(\phi_1-\phi_2)=180°$, once the magnetocrystal anisotropy of the Fe overlayer is accounted for. The existence of additional minima for $(\phi_1-\phi_2)=0$ or $(\phi_1-\phi_2)=180°$ stems from the fact that, for a weak AFM-FM coupling, the AFM spins can rearrange by unwinding the twisted AFM magnetic structure predicted by the proximity model,[11] confining the frustration at one of the AFM-FM interfaces.[12] The presence of a biquadratic term in the expression of the coupling energy is explained by the inequivalence between ±90° and 0° energy minima, which is a result of the different arrangement of the AFM local moments in different coupling configurations.[12]

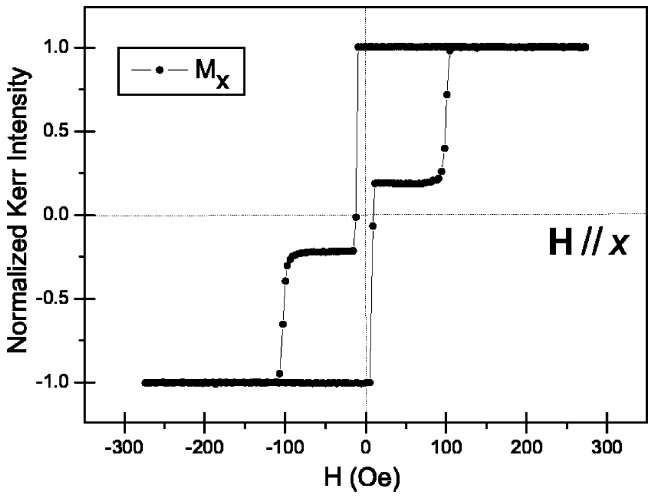

FIG. 6. Experimental longitudinal hysteresis loop for the Fe(70 Å)/NiO(100 Å)/Fe(3000 Å) trilayer ($\mathbf{H}\|x$). Loops have been normalized to unity.

It is interesting to note that the weight of the component proportional to $\sin^2[2(\phi_1-\phi_2)]$ is expected to be very small when the AFM thickness is below t_c,[12] in agreement with the observation that the K_4 value determined from the slope of the MOKE loop is about the same both in the Fe/NiO bilayer and in the Fe/NiO/Fe trilayer.

Finally, let us consider spacer thicknesses greater than t_c. The M_x hysteresis loop for the Fe(70 Å)/NiO(100 Å)/Fe(3000 Å) trilayer is shown in Fig. 6. It can be interpreted as the superposition of two square loops, the narrowest coming from the Fe substrate and the largest (coercivity of about 100 Oe) coming from the Fe overlayer contribution. For this trilayer no significant transverse component of the magnetization vector has been detected. Thus, no M_y loop is shown in the figures. The plateaux in the loop correspond then to a region where the magnetization vectors of the two layers are antiparallel, as they switch at different coercive fields, before becoming again parallel at higher values of the applied field.

We find that an increase in spacer thickness decreases the C_2 value, which is responsible for the perpendicular alignment of the magnetic layers: we can indeed fit our experimental data with $C_2=0$. The simulated loop for this trilayer

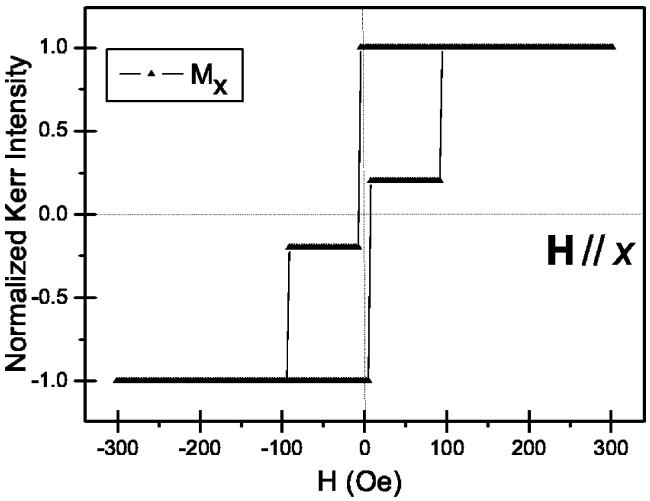

FIG. 7. Simulated longitudinal hysteresis loop for the Fe(70 Å)/NiO(100 Å)/Fe(3000 Å) trilayer ($\mathbf{H}\|x$). Loops have been normalized to unity.

is shown in Fig. 7. Again, no uniaxial term is necessary. It must be emphasized that, for trilayers with $t_{\mathrm{AFM}} > t_c$, there is a large uncertainty in the value of the fitting parameters. This is due to the fact that the bilinear coupling, the $\sin^2[2(\phi_1 - \phi_2)]$ coupling term, and the domain nucleation energy barriers have similar effects on the simulated hysteresis loops. In particular, increasing the values of any of these parameters results in increasing the coercive field of the overlayer. However, there is a limitation to the maximum value that can be attributed to C_1. In fact, at high C_1 values, the simulation predicts an antiparallel magnetic coupling between the FM layers at remanence, contrary to experimental evidence. It is remarkable that the C_1 value cannot be significantly higher than the maximum value that we have obtained for trilayers with $t_{\mathrm{AFM}} < t_c$. A very good fit of the coercive field can be obtained with $C_1 = 0$ and by an appropriate choice of the nucleation energy barriers and of the $\sin^2[2(\phi_1 - \phi_2)]$ term. As a final remark, we note that a decrease in the biquadratic coupling term accompanying a transition to collinear FM coupling is predicted by the extended proximity model presented in Ref. 12. The collinear coupling is, on the other hand, stabilized by the $\sin^2[2(\phi_1 - \phi_2)]$ term, which increases with the AFM spacer thickness.

IV. SPIN POLARIZED INVERSE PHOTOEMISSION

A. Experiments

As stated above, measurements exploiting spin-polarized electrons have also been performed on the samples as a preliminary study to build up a phase diagram describing the interlayer coupling behavior as a function of the NiO spacer and Fe overlayer thickness. The electron source is a GaAs photocathode, excited with circularly polarized light in order to get a spin polarized electron beam. Further details about the experimental setup have been reported elsewhere.[26,27] All measurements are taken with the samples magnetized at remanence, to avoid any interaction of the impinging electrons with the applied magnetic field. The low energy of the electron beam, between 5 and 20 eV, guarantees the low penetration depth of the probing electrons and thus the surface sensitivity of the measurements, giving information about the magnetic properties of the iron overlayer, with no contributions from the underlying layers.

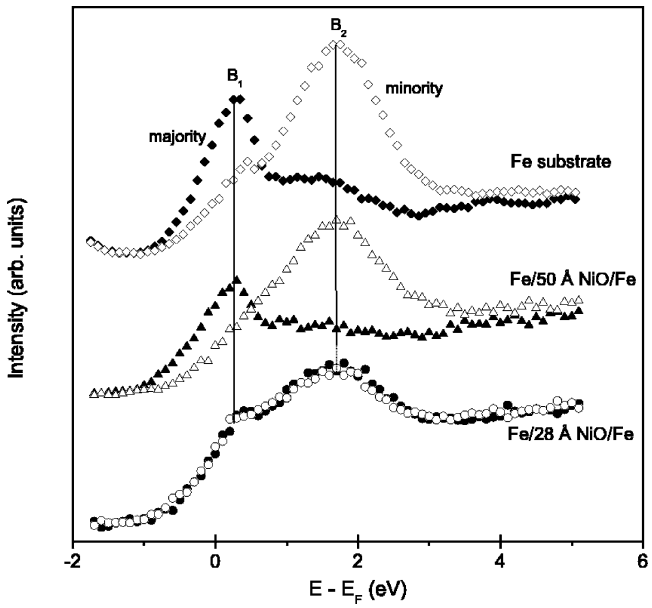

FIG. 8. Spin resolved inverse photoemission spectra of some Fe/NiO/Fe trilayers (central and lower panel) and of reference spectra from Fe substrate (upper panel). Full symbols relate to majority spin and open symbols to minority spin signals. All spectra are rescaled to 100 % electron beam polarization.

All SPIPE spectra are taken after having applied a 1400 Oe external magnetic field along the easy axis previously labeled as x axis. The magnitude of this field is greater than the saturation fields of both Fe substrate and overlayer, as confirmed by MOKE loops. In particular, due to the geometry of the experimental apparatus, the remanent magnetization of the overlayer can be detected along the same x axis.

B. Results and discussion

SPIPE allows one to obtain information on the magnetic properties of the trilayers analyzing the spin polarization dependence of the empty bands of the Fe overlayer. We have grown and investigated trilayers with many combinations of t_{AFM} and t_{over}. Typical SPIPE spectra for two trilayers are reported in Fig. 8, together with reference spectra from the substrate. Two features, labeled B_1 and B_2, are visible above E_F; they correspond to allowed transitions towards majority and minority final states, respectively.[17,28,29] The energy separation of the two peaks is correlated with the exchange splitting of bulk bands. It has indeed been observed in bulk Fe that such a splitting vanishes as the sample temperature approaches the Curie temperature, with the two peaks collapsing to a single band state.[29] Similar findings have been observed also on ultrathin Fe films.[27] The splitting is thus a signature of the presence of a FM order in the sample. In all the trilayers investigated such energy separation between the B_1 and B_2 peaks is unchanged: this indicates that the iron

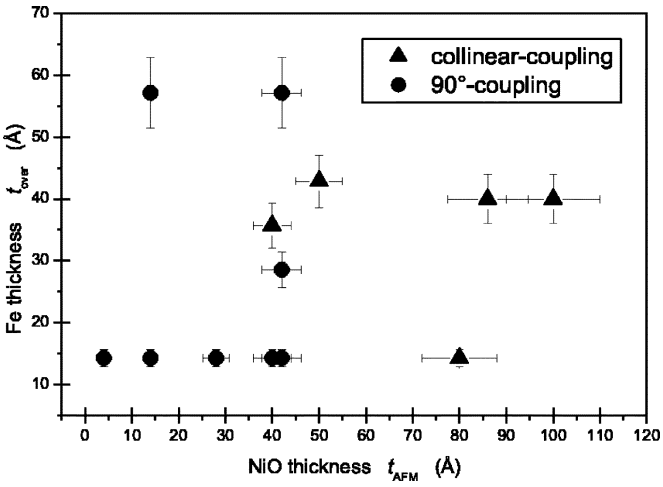

FIG. 9. Magnetization of Fe overlayer in Fe/NiO/Fe trilayers, as a function of t_{AFM} and t_{over}. Triangles relate to samples with an upper iron layer remanently magnetized along the direction of the applied field. Full circles relate to samples with zero net magnetization in that direction. Error bars are shown, corresponding to a general uncertainty of ±15% in both Fe and NiO thickness determination.

overlayer has, in any case, the same ferromagnetic properties as bulk Fe.

If one looks at the spin polarization dependence, however, dramatic changes can be seen as the NiO thickness increases. At small thicknesses (lower panel of Fig. 8), the spectra are completely unpolarized, while at larger thicknesses (central panel of Fig. 8) B_1 and B_2 appear in different spin channels. Note, as stated above, that we are sensitive only to the in-plane net magnetization along the x axis. Thus, if the sample is ferromagnetic but its net magnetization is directed perpendicularly with respect to that direction, no spin polarization effect will be observed in the inverse photoemission spectra.

When the net magnetization of the Fe overlayer is collinear with that of the Fe substrate, which is always parallel to the x axis, a strong polarization effect occurs. We refer to samples exhibiting such a behavior as "collinear-coupling" trilayers. When no polarization effect occurs, instead, we have zero remanent magnetization in the direction of the applied field which, on the basis of the MOKE results, we attribute to a perpendicular alignment of the overlayer remanent magnetization with respect to the Fe substrate. In this case we refer to "90°-coupling" trilayers.

Our results on several samples are summarized in Fig. 9, where triangles and full circles make reference to collinear-coupling and 90°-coupling trilayers, respectively. It is seen that all the samples with a t_{AFM} lower than about 40 Å are 90°-coupling trilayers in the sense illustrated above, while those with t_{AFM} larger than that value are collinear-coupling trilayers. An analysis of the error bars shown in Fig. 9 gives an uncertainty of approximately ±8 Å on the assessment of the t_c value.

The value $t_c \approx 40$ Å may be related to previous findings for similar systems. In the case of epitaxially grown $Fe_3O_4/NiO/Fe_3O_4$ trilayers,[8] a t_c of approximately 50 Å has been observed for the switching between perpendicular and parallel magnetic coupling, in close analogy with our result. In the extended proximity model, based on a coherent rotation of the spins in the FM and AFM layers,[12] an attempt to correlate the magnitude of the critical thickness for the transition between orthogonal and collinear coupling at zero applied field and the width of domain walls (δ_W) in the AFM spacer has been made, finding that the two quantities are of the same order of magnitude. The value of δ_W in bulk NiO single crystals has recently been measured and reported to vary between 134 and 184 nm.[30] If, following this interpretation, we compare these results to the t_c value that we found it is clear that our experimental value is considerably smaller. Such a mismatch is not surprising since coherent rotation models do not take into account the occurrence of defects either in the AFM volume, such as vacancies and dislocations,[31] or at the AFM-FM interface, such as interface roughness. Such defects are expected to reduce the coupling energy between the FM layers, with the result that t_c might be reduced considerably with respect to the δ_W value in the bulk AFM material. For instance, t_c cannot be expected to be larger than the characteristic distance between atomic steps at the AFM-FM interfaces.[32] Note that such interface and volume defects can have drastic effects at concentrations that are far below[33] the detection limit of photoemission and inverse photoemission techniques.

V. CONCLUSIONS

In summary, we have investigated the magnetization reversal processes of Fe/NiO/Fe(001) trilayers by means of SPIPE and MOKE measurements, obtaining evidence of two different behaviors, with a critical thickness of the NiO layer of about 40 Å for the transition between the two regimes. Below this value the relative alignment between the magnetization of the iron layers at zero applied field is perpendicular, while above this value it switches to collinear. This occurrence can be related to the active role of the antiferromagnetic spacer whose spin structure mediates the exchange coupling between the ferromagnetic layers. Simulations based on a biquadratic coupling term agree very well with the observed hysteresis loop, giving a confirmation of the proximity model extended to the low AFM-FM interface coupling case. We find that the biquadratic coupling disappears for $t_{AFM} > 40$ Å.

ACKNOWLEDGMENTS

The authors would like to thank Ezio Puppin for valuable assistance in the MOKE experiments. A. Schmid and N. Rougemaille are also gratefully acknowledged for fruitful discussions.

*Electronic address: alberto.brambilla@polimi.it
†Also at INFM, Dipartimento di Fisica, Politecnico di Milano, Piazza Leonardo Da Vinci 32, 20133 Milano, Italy.

[1] See, e.g., P. Grünberg, Phys. Today **54** (5), 31 (2001); G. A. Prinz, J. Magn. Magn. Mater. **200**, 57 (1999).
[2] For reviews see, e.g., J. Nogués and I. K. Schuller, J. Magn. Magn. Mater. **192**, 203 (1999); A. E. Berkowitz and K. Takano, *ibid.* **200**, 552 (1999).
[3] O. Zaharko, P. M. Oppeneer, H. Grimmer, M. Horisberger, H.-Ch. Mertins, D. Abramsohn, F. Schäfers, A. Bill, and H.-B. Braun, Phys. Rev. B **66**, 134406 (2002).
[4] A. S. Edelstein, R. H. Kodama, M. Miller, V. Browning, P. Lubitz, S. F. Cheng, and H. Sieber, Appl. Phys. Lett. **74** 3872 (1999).
[5] M. E. Filipkowski, J. J. Krebs, G. A. Prinz, and C. J. Gutierrez, Phys. Rev. Lett. **75**, 1847 (1995).
[6] A. Azevedo, C. Chesman, S. M. Rezende, F. M. de Aguiar, X. Bian, and S. S. P. Parkin, Phys. Rev. Lett. **76**, 4837 (1996).
[7] P. Vavassori, M. Grimsditch, and E. E. Fullerton, J. Magn. Magn. Mater. **223**, 284 (2001).
[8] P. A. A. van der Heijden, C. H. W. Swüste, W. J. M. de Jonge, J. M. Gaines, J. T. W. M. van Eemeren, and K. M. Schep, Phys. Rev. Lett. **82**, 1020 (1999).
[9] J. Camarero, Y. Pennec, J. Vogel, M. Bonfim, S. Pizzini, F. Ernult, F. Fettar, F. Garcia, F. Lançon, L. Billard, B. Dieny, A. Tagliaferri, and N. B. Brookes, Phys. Rev. Lett. **91**, 027201 (2003).
[10] S. O. Demokritov, J. Phys. D **31**, 925 (1998).
[11] J. C. Slonczewski, J. Magn. Magn. Mater. **150**, 13 (1995).
[12] H. Xi and R. M. White, Phys. Rev. B **62**, 3933 (2000).
[13] T. J. Regan, H. Ohldag, C. Stamm, F. Nolting, J. Lüning, J. Stöhr, and R. L. White, Phys. Rev. B **64**, 214422 (2001).
[14] M. Finazzi, M. Portalupi, A. Brambilla, L. Duò, G. Ghiringhelli, F. Parmigiani, M. Zacchigna, M. Zangrando, and F. Ciccacci, Phys. Rev. B **69**, 014410 (2004).
[15] M. Finazzi, A. Brambilla, L. Duò, G. Ghiringhelli, M. Portalupi, F. Ciccacci, M. Zacchigna, and M. Zangrando, Phys. Rev. B **70**, 235420 (2004).
[16] R. Bertacco, S. De Rossi, and F. Ciccacci, J. Vac. Sci. Technol. A **16**, 2277 (1998).
[17] R. Bertacco and F. Ciccacci, Phys. Rev. B **59**, 4207 (1999).
[18] L. Duò, M. Portalupi, M. Marcon, R. Bertacco, and F. Ciccacci, Surf. Sci. **518**, 234 (2002).
[19] D. Alders, L. H. Tjeng, F. C. Voogt, T. Hibma, G. A. Sawatzky, C. T. Chen, J. Vogel, M. Sacchi, and S. Iacobucci, Phys. Rev. B **57**, 11623 (1998).
[20] P. Vavassori, Appl. Phys. Lett. **77**, 1605 (2000); E. Puppin, P. Vavassori, and L. Callegaro, Rev. Sci. Instrum. **71**, 1752 (2000).
[21] J. Camarero, Y. Pennec, J. Vogel, M. Bonfim, S. Pizzini, M. Cartier, F. Ernult, F. Fettar, and B. Dieny, Phys. Rev. B **64**, 172402 (2001).
[22] R. P. Cowburn, S. J. Gray, J. Ferré, J. A. C. Bland, and J. Miltat, J. Appl. Phys. **78**, 7210 (1995).
[23] M. Cartier, S. Auffret, Y. Samson, P. Bayle-Guillemaud, and B. Dieny, J. Magn. Magn. Mater. **223**, 63 (2001).
[24] M. Zangrando, M. Finazzi, G. Paolucci, G. Comelli, B. Diviacco, R. P. Walker, D. Cocco, and F. Parmigiani, Rev. Sci. Instrum. **72**, 1313 (2001); M. Zangrando, M. Finazzi, M. Zacchigna, D. Cocco, R. Rochow, and F. Parmigiani, *ibid.* **75**, 31 (2004).
[25] Inequivalence between the $(\phi_1-\phi_2)=0$ and $(\phi_1-\phi_2)=\pm 180°$ minima can be expected in the case of exchanged biased AFM-FM interfaces. This inequivalence can be accounted for by an additional bilinear term. See Refs. 11 and 12.
[26] F. Ciccacci, S. De Rossi, E. Pelucchi, and A. Tagliaferri, Rev. Sci. Instrum. **68** 1841 (1997).
[27] G. Chiaia, S. De Rossi, L. Mazzolari, and F. Ciccacci, Phys. Rev. B **48**, 11298 (1993).
[28] A. Santoni and F. J. Himpsel, Phys. Rev. B **43**, 1305 (1991).
[29] J. Kirschner, M. Glöbl, V. Dose, and H. Scheidt, Phys. Rev. Lett. **53**, 612 (1984).
[30] N. B. Weber, H. Ohldag, H. Gomonaj, and F. U. Hillebrecht, Phys. Rev. Lett. **91**, 237205 (2003).
[31] M. Finazzi, P. Biagioni, A. Brambilla, L. Duò, and F. Ciccacci, Phys. Rev. B **72**, 024410 (2005).
[32] A. I. Morosov and A. S. Sigov, Fiz. Tverd. Tela (S.-Peterburg) **46**, 385 (2004) [Phys. Solid State **46**, 395 (2004)].
[33] P. Miltényi, M. Gierlings, J. Keller, B. Beschoten, G. Güntherodt, U. Nowak, and K. D. Usadel, Phys. Rev. Lett. **84**, 4224 (2000).